



Gravitational Waves from Merging Intermediate-mass Black Holes.

II. Event Rates at Ground-based Detectors

Hisa-aki Shinkai¹, Nobuyuki Kanda², and Toshikazu Ebisuzaki³

¹ Dept. of Information Science and Technology, Osaka Institute of Technology, Kitayama 1-79-1, Hirakata City, Osaka 573-0196, Japan; hisaaki.shinkai@oit.ac.jp

² Dept. of Physics, Osaka City University, Sugimoto 3-3-138, Sumiyoshi, Osaka City, Osaka 558-8585, Japan; kanda@sci.osaka-cu.ac.jp

³ Computational Astrophysics Laboratory, Institute of Physical and Chemical Research (RIKEN), Hirosawa 2-1, Wako City, Saitama 351-0198, Japan; ebisu@riken.jp

Received 2016 October 28; revised 2016 December 12; accepted 2016 December 22; published 2017 February 1

Abstract

Based on a dynamical formation model of a supermassive black hole (SMBH), we estimate the expected observational profile of gravitational waves at ground-based detectors, such as KAGRA or advanced LIGO/VIRGO. Noting that the second generation of detectors have enough sensitivity from 10 Hz and up (especially with KAGRA owing to its location at less seismic noise), we are able to detect the ring-down gravitational wave of a BH with mass $M < 2 \times 10^3 M_\odot$. This enables us to check the sequence of BH mergers to SMBHs via intermediate-mass BHs. We estimate the number density of galaxies from the halo formation model and estimate the number of BH mergers from the giant molecular cloud model assuming hierarchical growth of merged cores. At the designed KAGRA (and/or advanced LIGO/VIRGO), we find that the BH merger of its total mass $M \sim 60 M_\odot$ is at the peak of the expected mass distribution. With its signal-to-noise ratio $\rho = 10(30)$, we estimate the event rate $R \sim 200(20)$ per year in the most optimistic case, and we also find that BH mergers in the range $M < 150 M_\odot$ are $R > 1$ per year for $\rho = 10$. Thus, if we observe a BH with more than $100 M_\odot$ in future gravitational-wave observations, our model naturally explains its source.

Key words: globular clusters: general – gravitational waves – quasars: supermassive black holes – stars: black holes

1. Introduction

1.1. Era of Gravitational-wave Astronomy

The direct detections of gravitational waves were announced by the advanced LIGO group in 2016 (Abbott et al. 2016a, 2016b), and we are at the opening era of “gravitational-wave astronomy.” The LIGO group reported two events (GW150914, GW151226) and one transient event (LVT151012), all three of which are regarded as events of coalescence of binary black holes (BBHs).

The first event (GW150914) was the merger of BHs of masses $36.2^{+5.2}_{-3.8} M_\odot$ and $29.1^{+3.7}_{-4.4} M_\odot$, which turned into a single BH of $62.3^{+3.7}_{-3.1} M_\odot$ with spin $a = 0.68^{+0.05}_{-0.06}$, which shows that the energy radiation rate is 4.6% of the total mass. The event occurred at redshift $z = 0.09^{+0.03}_{-0.04}$ and was detected with signal-to-noise ratio (S/N) $\rho = 23.7$. The second event (GW151226) was the merger of BHs with $14.2^{+8.3}_{-3.7} M_\odot$ and $7.5^{+2.3}_{-2.3} M_\odot$, which turned into a single BH of $20.8^{+6.1}_{-1.7} M_\odot$ with spin $a = 0.74^{+0.06}_{-0.06}$, which shows that the energy radiation rate is 4.1% of the total mass. The event occurred at redshift $z = 0.09^{+0.03}_{-0.04}$ and was detected with $\rho = 13.0$ (these numbers were taken from Abbott et al. 2016c).

These announcements were not only valuable on the point of the direct detections of the gravitational wave, but also the first results confirming the existence of BHs, the existence of BHs of this mass range, and the existence of BBHs. Especially, the existence of $\sim 30 M_\odot$ BHs was surprising to the community, since there were no such observational evidences ever before.

1.2. Possible Sources of $30 M_\odot$ BHs

The traditional scenarios for forming BBHs are common envelope evolution of primordial binary massive stars

(Belczynski et al. 2016) and dynamical formation in dense star clusters (Portegies Zwart & McMillan 2000).

One possible scenario is to suppose that BBHs form from Population III stars (Bond Carr 1984, Belczynski 2004). Recently, Kinugawa (2014, 2016) predicted event rates based on this model. Existence of Population III stars is yet to be confirmed, but they show that a typical BH mass of this model is at $\sim 30 M_\odot$ (chirp mass $\sim 60 M_\odot$), and the event rate would be 500 yr^{-1} (50 yr^{-1} for $\rho \geq 20$; Nakano et al. 2015).

Recently, M. S. Fujii et al. (2016, in preparation) estimate BH mergers combining their N -body simulations, modeling of globular clusters, and cosmic star-cluster formation history and find that BH mass distribution has a peak at $10 M_\odot$ and $50 M_\odot$, and the event rate for designed LIGO is at most 85 yr^{-1} .

In this article, based on the formation scenario of a supermassive BH (SMBH), we extend the previous model to a sequence of intermediate-mass BHs (IMBHs) and estimate their observational detectability at ground-based gravitational-wave detectors.

1.3. SMBH Runaway Path

The formation process of an SMBH is one of the unsolved problems in galaxy evolution history. Many possible routes were suggested by Rees (1978) long ago, but we still debate a plausible route. We do not yet know whether the first generation of BHs are of stellar-mass size or supermassive. See, e.g., Volonteri (2012) and Haiman (2013) for a review.

One of the simplest scenarios for forming an SMBH is from the direct collapse of gas clouds or supermassive stars, or massive disks (e.g., Umemura et al. 1993; Loeb & Rasio 1994; Shibata & Shapiro 2002; Bromm & Loeb 2004; Begelman

et al. 2006, 2008). Another scenario is by accretions onto, or mergers of, the remnants of Population III stars (e.g., Haiman & Loeb 2001; Volonteri & Begelman 2010; Johnson et al. 2012, 2013). Recent studies suggest that we can construct a formation route of SMBHs without contradicting with current observations.

In this article, we take the third route: accumulations of BHs. This route came to be believed when an IMBH (10^2 – $10^3 M_\odot$) was first discovered in starburst galaxy M82 (Matsumoto et al. 2001; Matsushita et al. 2000). So far, many IMBHs have been found in the center of galaxies (for a review, see, e.g., Greene 2012; Yagi 2012), and also the existence of an IMBH of $10^4 M_\odot$ close to Sgr A* has recently been reported (Tsuboi et al. 2016; see also Portegies Zwart et al. 2006; Fujii et al. 2008).

This runaway path was first proposed by Ebisuzaki et al. (2001). The scenario consists of three steps: (1) formation of IMBHs by runaway mergers of massive stars in dense star clusters (Portegies Zwart et al. 2004), (2) accumulations of IMBHs at the center region of a galaxy due to sinkages of clusters by dynamical friction, and (3) mergers of IMBHs by multibody interactions and gravitational radiation. Successive mergers of IMBHs are likely to form an SMBH with a mass $> 10^6 M_\odot$. Ebisuzaki et al. (2001) predicted that IMBH–IMBH or IMBH–SMBH merging events could be observed on the order of one per month or even one per week.

Numerical simulations support the above first step (Marchant & Shapiro 1980; Portegies Zwart et al. 1999; Portegies Zwart & McMillan 2002; Portegies Zwart et al. 2004; Baumgardt & Makino 2003), and the second step is also confirmed in a realistic mass-loss model (Matsubayashi et al. 2007), while the third step is not yet investigated in detail. The discovery of an SMBH binary system (Sudou et al. 2003), together with a simulation of an eccentric evolution of SMBH binaries (Iwasawa et al. 2010), supports this formation scenario through merging of IMBHs.

1.4. IMBHs and Gravitational Waves

In Matsubayashi et al. (2004, hereafter Paper I), we pointed out that gravitational waves from IMBHs can be a trigger to prove this process. If the space-based laser interferometers are in action, then their observation ranges (10^{-4} –10 Hz) are quite reasonable for IMBH mergers. By accumulating data of merger events, we can specify the IMBH merger scenario such as they merge hierarchically or monopolistically.

Later, Fregeau et al. (2006) discussed the event rates of IMBH–IMBH binary observations at advanced LIGO and VIRGO and concluded that we can expect ~ 10 mergers per year. This work was followed by Gair et al. (2011), including the Einstein Telescope project. Amaro-Seoane & Santamaría (2010) also discussed the IMBH–IMBH system, including the pre-merger phase.

Noting that the second generation of GW interferometers have enough sensitivity at 10 Hz and above (see Figure 1), we are able to detect the ring-down gravitational wave of a BH of mass $M < 2 \times 10^3 M_\odot$.

In this article, we therefore discuss how much we can observe BH mergers by finding their ring-down part using designed ground-based detectors. We roughly assume the mass distribution of BHs, $N(M)$, in a galaxy or globular cluster, which would be related to the merging history of BHs, and estimate the event rate using the designed strain noise of

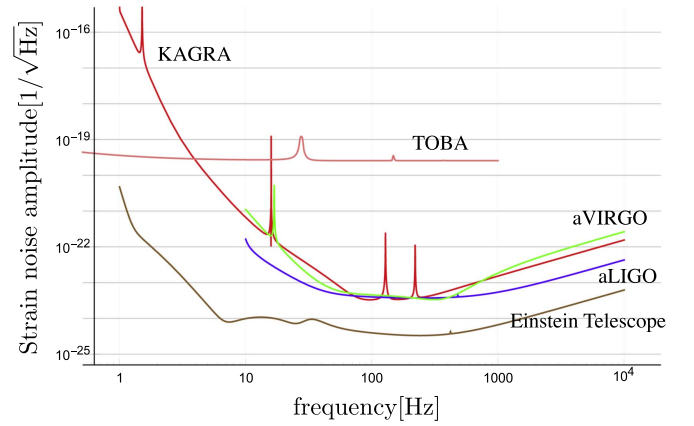


Figure 1. Designed strain noise amplitude of the advanced detectors (advanced LIGO, advanced VIRGO, and KAGRA) and the planned Einstein Telescope. We also plotted that of a torsion-bar antenna (TOBA).

KAGRA, which is at the equivalent level with aLIGO/aVIRGO.

In addition, recent approaches to gravitational-wave detection using a torsion-bar antenna (TOBA; Ando et al. 2010; Ishidoshiro et al. 2011) are also quite attractive for this purpose since it covers the low frequency range (0.1–10 Hz). However, the current strain noise amplitude of TOBA is larger compared to those of interferometers (see Figure 1), and we do not discuss the case of TOBA in this article.

The organization of the paper is as follows. In Section 2, we present the basic equations of gravitational radiation from IMBH binaries. In Section 3, we estimate the event rate of IMBH mergers under the simplest assumptions on the galaxy distribution and formation process of SMBHs. A summary and discussion are presented in Section 4. Throughout the paper, we use c and G for the light speed and gravitational constant, respectively.

2. Black Hole Merger Model

2.1. Ring-down Frequency from BHs

The gravitational waveform of binary-star mergers, which ends up with a single BH, has three typical phases: inspiral phase, merging phase, and ring-down phase. The waveform in the inspiral phase is called the “chirp signal” from its feature of increasing frequency and amplitude. For the case of GW150914, the frequency was first caught at 35 Hz, and then it increased to 150 Hz, where the amplitude reached the maximum, which indicates the merger of the binary. The final “ring-down” signal was supposed to be around 300 Hz.

As we mentioned in Paper I, for massive BH binaries with masses greater than $10^3 M_\odot$, the inspiral frequencies are less than 1 Hz. The wavelength of this frequency range is apparently more than the size of Earth, so that its detection requires interferometers in space. On the other hand, the ring-down frequency is simply estimated by the quasi-normal frequency of BHs, $f_R + if_I$, which is determined from the mass and spin of the final BH and is estimated to be higher than in its inspiral phase. The quasi-normal modes are derived as eigenvalues of the wave equations on the perturbed geometry (see, e.g., Leaver 1985). For a BH with mass M_T and spin a , fitting functions are also known (Echeverria 1980; Berti et al.

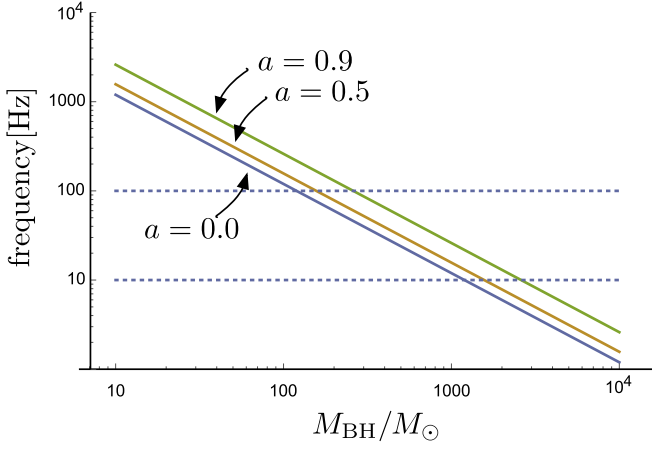


Figure 2. Quasi-normal frequency f_{qnm} as a function of the mass of BHs M_T . If we restrict the observable range to above 10 Hz for the advanced ground-based interferometers, then the BHs with mass less than $2000 M_\odot$ are within the target.

2006) in the form

$$f_R = f_1 + f_2(1 - a)^{f_3}, \quad (1)$$

$$Q \equiv \frac{f_R}{2f_1} = q_1 + q_2(1 - a)^{q_3}, \quad (2)$$

where Q is called the quality factor and f_i, q_i are fitting coefficients. For the most fundamental mode, which is of the spherical harmonic index $\ell = 2, m = 2$, the fitting parameters are $f_1 = 1.5251, f_2 = -1.1568, f_3 = 0.1292, q_1 = 0.7000, q_2 = 1.4187$, and $q_3 = -0.4990$ (Berti et al. 2006). Recovering the units, we can write the frequency as

$$\begin{aligned} f_{\text{qnm}} &= \frac{c^3}{2\pi G M_T} f_R \\ &\sim 3.2 \left(\frac{10 M_\odot}{M_T} \right) f_R [\text{kHz}]. \end{aligned} \quad (3)$$

We plot f_{qnm} in Figure 2.

Supposing that advanced GW interferometers can detect f_{qnm} above 10 Hz, then BHs less than $1200 M_\odot$ are within the target if BHs are nonrotating ($a = 0$), while BHs less than $2500 M_\odot$ are in the detectable range for highly rotating cases ($a = 0.98$).

With this simple estimation, we hereafter consider mergers of BHs with total mass less than $2000 M_\odot$.

2.2. Number of Galaxies in the Universe

In order to model the typical mass of galaxies and its distribution, we apply the halo mass function given by Vale & Ostriker (2006), in which they discuss an empirically based, nonparametric model for galaxy luminosities with halo/subhalo masses. They apply the Sheth–Tormen mass function (Sheth & Tormen 1999) for halo number density,

$$n_H(M) dM = 0.322 \left(1 + \frac{1}{\nu^{0.6}} \right) \sqrt{\frac{2}{\pi}} \frac{d\nu}{dM} \exp\left(-\frac{\nu^2}{2}\right) dM, \quad (4)$$

where $\nu = \sqrt{a} \delta_c (1 + z) \sigma(M)$ with $a = 0.707$, the linear threshold for spherical collapse $\delta_c = 1.686$, and $\sigma(M)$ is the variance on the mass scale M . This mass function is roughly $\sim M^{-1.95}$ at low mass.

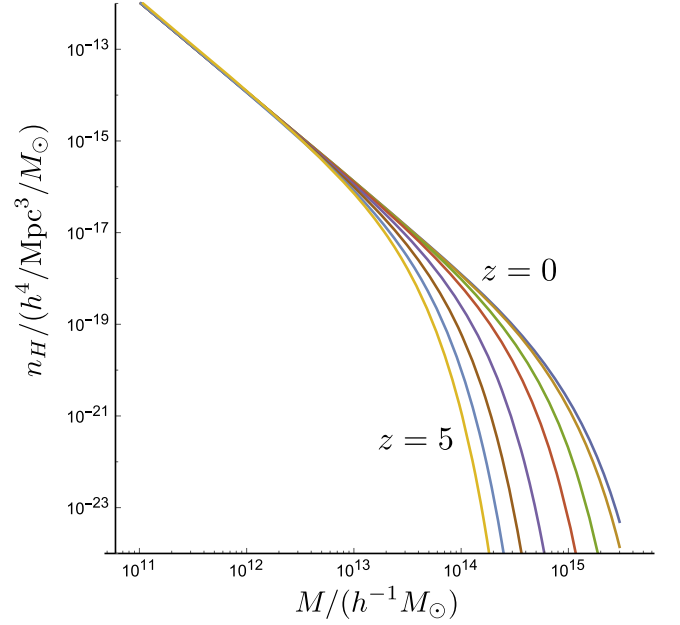


Figure 3. Global mass functions for halos (halo and subhalo), $n_H(M)$, for $z = 0, 0.1, 0.5, 2, 4, 5$ (Equation (4)). $n_H(M)$ is in units of $h^4/\text{Mpc}^3/M_\odot$. M is in units of $h^{-1}M_\odot$, with $h = 0.7$.

Vale & Ostriker (2006) also derive an average number of galaxies (subhalos) predicted for a parent halo of mass, which is roughly given by $N_{\text{subhalo}} \sim M^{0.9}$ (Figure 12 in their paper). If we regard this relation as a seed of galaxies, then it indicates that a typical galaxy has mass $10^{11} - 10^{12} M_\odot$.

Integrating Equation (4) by the volume as a function of redshift z , we can derive the number density of halos (Figure 3). In this process, we use the standard cosmology model with current parameters, i.e., we use the flat Friedmann model with Hubble constant $H_0 = 72 \text{ km s}^{-1} \text{ Mpc}^{-1}$, matter and dark matter density $\Omega_{m0} = 0.27$, and dark energy (cosmological constant) $\Omega_{d0} = 0.73$. The luminosity distance $d_L(z)$ is given by

$$d_L(z) = (1 + z) \int_0^z \frac{c dz}{H(z)}, \quad (5)$$

where

$$H(z) = H_0 \sqrt{(1 + z)^3 \Omega_{m0} + \Omega_{d0}}. \quad (6)$$

The volume of the universe is $V(d) = 4\pi d^3/3$.

Combining these two functions (average number of galaxies and the number density of halos), we get the number density of galaxies $n_{\text{galaxy}}(M, z)$, which we show in Figure 4. If we integrate it by M and z as

$$N_{\text{galaxy}}(z) = \int_0^z dz \int_{M_1}^{M_2} n_{\text{galaxy}}(M, z) dM, \quad (7)$$

then we get the number of galaxies. We set $M_1 = 10^9 M_\odot$ and $M_2 = 10^{13} M_\odot$.

From the recent ultraviolet luminosity density of star-forming galaxies, star formation rate density $\rho_{\text{SFR}}(z)$ is fit as

$$\rho_{\text{SFRp}}(z) = \frac{0.009 + 0.27(z/3.7)^{2.5}}{1 + (z/3.7)^{7.4}} + 10^{-3}, \quad (8)$$

$$\rho_{\text{SFRr}}(z) = \frac{0.009 + 0.27(z/3.4)^{2.5}}{1 + (z/3.4)^{8.3}} + 10^{-4}, \quad (9)$$

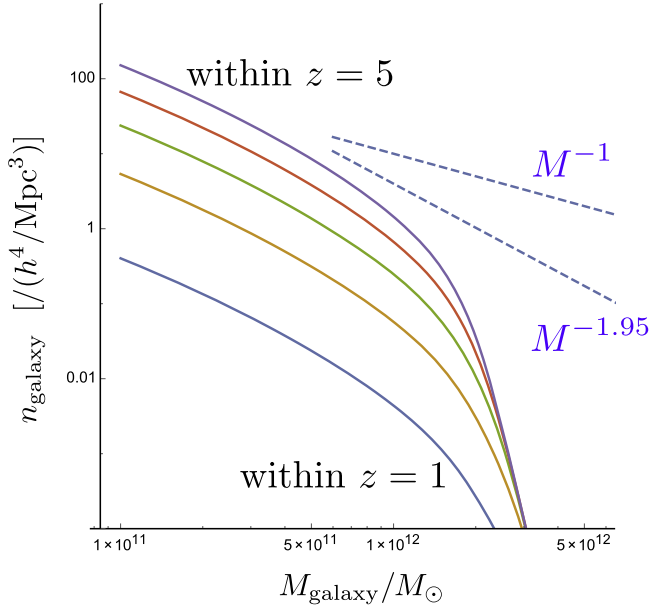


Figure 4. Number density of galaxies, $n_{\text{galaxy}}(M)$.

for metal-poor stars and metal-rich stars, respectively (Robertson et al. 2010). If we sum these two (normalized ρ_{SFRp} and normalized ρ_{SFRr}) evenly, the peak location is at $z = 3.26$. We then obtain

$$N_{\text{galaxy}}(z) = \int_0^z \rho_{\text{SFR}}(z) dz \int_{M_1}^{M_2} n_{\text{galaxy}}(M, z) dM. \quad (10)$$

The typical numbers of our model are shown in Table 1. These numbers are slightly larger than the latest observation by Conselice et al. (2016), but our model produces the same order and evolution history for N_{galaxy} as theirs.

2.3. Number of BHs in a Galaxy

We next estimate the number of BH candidates in a galaxy. Recently, Inutsuka et al. (2015) developed a scenario of galactic-scale star formation from a giant molecular cloud. Their model includes both the growth of molecular clouds and the destruction of magnetized molecular clouds by radiation. Simulations and steady-state analysis show that the mass density function of molecular clouds, $n_{\text{cl}}(M_{\text{cl}})$, converges at the Schechter-like function,

$$n_{\text{cl}}(M_{\text{cl}}) \sim M_{\text{cl}}^{-1.7} \exp\left(-\frac{M_{\text{cl}}}{M_{\text{cut}}}\right), \quad (11)$$

where the cutoff mass $M_{\text{cut}} = 10^6 M_{\odot}$.

On the other hand, many N -body simulations report that there is a simple relation between the mass of the most massive cluster m_{max} and the total mass of the molecular cloud M_{cl} ,

$$m_{\text{max}} = 0.20 M_{\text{cl}}^{0.76}. \quad (12)$$

The single-line fit can be seen for the wide range $M_{\text{cl}}/M_{\odot} = 10^0$ – 10^7 (see Figure 6 in Fujii & Portegies Zwart 2015).

We therefore combine these results, and we suppose that each molecular cloud forms a single BH in its core if it is more than $10 M_{\odot}$, and we suppose that these BHs become ‘‘building blocks’’ for forming stellar-sized and intermediate-mass BHs. Many N -body simulations suggest that massive objects will

Table 1

Typical Numbers of Our Galaxy Model: Number of Galaxies $N_{\text{galaxy}}(z)$, Equation (10), and Number Density of Galaxies n_{galaxy}

z	$N_{\text{galaxy}}(z)$	n_{galaxy}	
1	1.18×10^9	$1.0 \times 10^{-3}/\text{Mpc}^3$	for $z < 1$
2	9.45×10^{10}	$6.5 \times 10^{-3}/\text{Mpc}^3$	for $1 < z < 2$
3	5.23×10^{12}	$2.4 \times 10^{-2}/\text{Mpc}^3$	for $2 < z < 3$

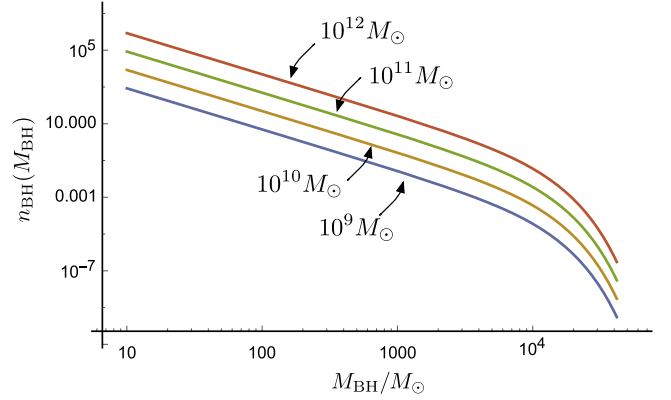


Figure 5. Number density of BHs per galaxy as a function of BH mass for different total mass of galaxies $M_{\text{galaxy}} = 10^9 M_{\odot}, \dots, 10^{12} M_{\odot}$.

accumulate in the center of a galaxy owing to dynamical friction, so that we modeled that these seed BHs accumulate and merge repeatedly (as we model below), resulting in IMBHs and SMBHs. We do not specify where these mergers occur, but we count our BH mergers after we set up the initial seeds. We show the number density of BHs in a galaxy, $n_{\text{BH}}(M_{\text{BH}})$, in Figure 5.

2.4. Number of BH Mergers in a Galaxy

In Paper I, we considered two toy models for formation of SMBHs: hierarchical growth and runaway growth. The hierarchical growth model is the case in which two nearby equal-mass BHs merge simultaneously and continue their mergers. The runaway growth model is, conversely, where only one BH grows itself by continual mergers with surrounding BH companions.

The recent N -body simulations report that the hierarchical merger process is plausible both for the massive clusters (10^4 – $10^6 M_{\odot}$; see, e.g., Fujii & Portegies Zwart 2015) and for stellar-mass BHs (see, e.g., M. S. Fujii et al. 2016, in preparation).

We therefore simply assume that BHs formed at cores of clouds will accumulate each other hierarchically, i.e., the mass and the number of BHs at steps from k to $k + 1$ can be expressed simply by

$$M_{k+1} = 2M_k, \quad (13)$$

$$N_{k+1} = N_k/2. \quad (14)$$

The mass of a BH merger, then, obeys the distribution M^{-1} .⁴

⁴ Suppose we have a cluster of total mass M_c that consists of N_0 equal-mass BHs. This means that each BH mass is initially M_c/N_0 . They continue to form binaries and merge together, which indicates that there are $N_0/2^{i-1}$ binaries for the i th generation that forms BHs with masses $M = 2^{i-1}M_c/N_0$. The model shows only the discrete distribution of the BH mass, but the number of binaries $N(M)$ can be approximated with the number of initial fractions in a cluster, $N(M) = M_c/M$.

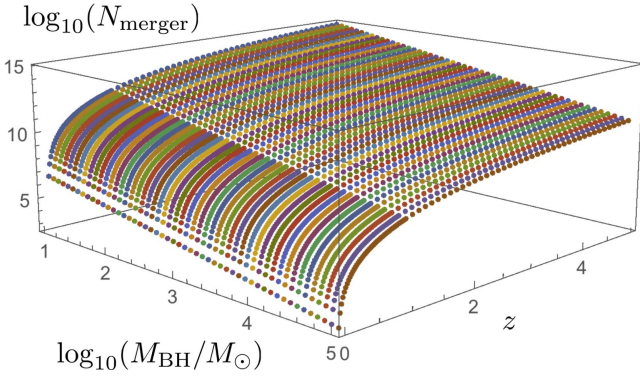


Figure 6. Cumulative distribution function of the number of BH mergers $N_{\text{merger}}(M_{\text{BH}})$ as a function of the redshift z . N_{merger} is expressed with binned one, of which we binned 20 for one order in M_{BH} .

On the other hand, we know empirically that the mass of the central BH of the galaxy, M_{SMBH} , and the total mass of the galaxy, M_{galaxy} , has a relation

$$M_{\text{SMBH}} = 2 \times 10^{-4} M_{\text{galaxy}} \quad (15)$$

(or equal to 10^{-3} of the bulge mass; see, e.g., King 2003; McConnell & Ma 2013).

Combining these facts, for a certain galaxy with M_{galaxy} , we pick up BHs with total mass M_{SMBH} (equation above), obeying the mass distribution of Figure 5. We suppose that picked-up BHs will form an SMBH in its series of mergers in the hierarchical model. Together with galaxy distribution function $n_{\text{galaxy}}(M, z)$, we are able to count the possible events of BH mergers, $N_{\text{merger}}(M_{\text{BH}}, z)$, in the universe, which we show in Figure 6.

In the next section, we further take into account the detectors' detectable distance $D(M, a, \rho)$ (with BH spin parameter a , energy emission rate of merger, and S/N ρ). In Section 4, we estimate the observable event rate,

$$\text{Event Rate } R[\text{/yr}] = \frac{N_{\text{merger}}(z)}{V(D/2.26)}, \quad (16)$$

where the factor 2.26 is for averaging the distance for all directions (Finn & Chernoff 1993).

3. Signal-to-noise Ratio and Detectable Distance

3.1. S/N

Let the true signal $h(t)$, the function of time, be detected as a signal, $s(t)$, which also includes the unknown noise, $n(t)$:

$$s(t) = h(t) + n(t). \quad (17)$$

The standard procedure for the detection is judged by the optimal S/N, ρ , which is given by

$$\rho = 2 \left[\int_0^\infty \frac{\tilde{h}(f)\tilde{h}^*(f)}{S_n(f)} df \right]^{1/2}, \quad (18)$$

where $\tilde{h}(f)$ is the Fourier-transformed quantity of the wave,

$$\tilde{h}(f) = \int_{-\infty}^\infty e^{2\pi ift} h(t) dt, \quad (19)$$

and $S_n(f)$ is the (one-sided) power spectral density of strain noise of the detector, as we showed in Figure 1. In this paper,

for KAGRA (bKAGRA), we use a fitted function

$$\sqrt{S_n(f)} = 10^{-26} \left(\frac{6.5 \times 10^{10}}{f^8} + \frac{6 \times 10^6}{f^{2.3}} + 1.5f \right), \quad (20)$$

where f is measured in Hz, as was used in Nakano et al. (2015).

3.2. S/N of Ring-down Wave

For the ring-down gravitational wave in the presence of a BH, the waveform is modeled as

$$h(t) = A \cos(2\pi f_R(t - t_0) + \psi_0) e^{-(t-t_0)/\tau}, \quad (21)$$

where f_R is the oscillation frequency, τ is the decaying time constant, and t_0 and ψ_0 are the initial time and its phase, respectively (we simply set $t_0 = \psi_0 = 0$). The parameter τ is normally expressed using a quality factor, $Q \equiv \pi f_R \tau$, or $f_I = 1/(2\pi\tau)$. The waveform, Equation (21), is then written as

$$h(t) \sim A e^{i2\pi(f_R + if_I)t}, \quad (22)$$

where we call $f_R + if_I$ the quasi-normal frequency, which is obtained from the perturbation analysis of BHs, and its fitting equations are shown in Equation (3).

Following Flanagan & Hughes (1998), we use the energy spectrum formula for the ring-down wave,

$$\begin{aligned} \frac{dE}{df} &= \frac{A^2 M^2 f^2}{32\pi^3 \tau^2} \\ &\times \left\{ \frac{1}{[(f - f_R)^2 + f_I^2]^2} + \frac{1}{[(f + f_R)^2 + f_I^2]^2} \right\} \\ &\approx \frac{1}{8} A^2 M^2 f_R Q \delta(f - f_R) [1 + O(1/Q)], \end{aligned} \quad (23)$$

where M is the total mass of the binary, $M = m_1 + m_2$.

We then obtain

$$E_{\text{ringdown}} \approx \frac{1}{8} A^2 M^2 f_R Q. \quad (24)$$

Let $\epsilon_r(a) \equiv E_{\text{ringdown}}/M$, which expresses the energy fraction of the emitted gravitational wave to the total mass. As we cited in the introduction, GW150914 and GW151226 show us $a = 0.67$ and 0.74 and energy emission rate 4.6% and 4.1% of the total mass, respectively. The associated numerical simulation of GW150914 (SXS:BBH:0305)⁵ shows that 4.0% of the total mass is emitted before the merger.⁶ That is, the ring-down part emits the energy around 0.6% of the total mass. If we use $A \sim 0.4$, then we recover the ratio $\epsilon_r(0.67) = 0.58\%$ (it also produces, e.g., $\epsilon_r(0.0) = 0.236\%$, $\epsilon_r(0.5) = 0.425\%$, $\epsilon_r(0.9) = 1.23\%$, $\epsilon_r(0.98) = 2.98\%$). The magnitude of this A is also consistent with the quadrupole formula.

The S/N is, then, expressed using the inertial mass $\mu = m_1 m_2 / M$ and the redshift of the source z ,

$$\begin{aligned} \rho^2 &= \frac{8}{5} \frac{\epsilon_r(a)}{f_R^2} \frac{(1+z)M}{S_h(f_R/(1+z))} \\ &\times \left(\frac{(1+z)M}{d_L(z)} \right)^2 \left(\frac{4\mu}{M} \right)^2. \end{aligned} \quad (25)$$

⁵ SXS Gravitational Waveform Database (<https://www.black-holes.org/waveforms/>).

⁶ We thank Hiroyuki Nakano for pointing out this ratio.

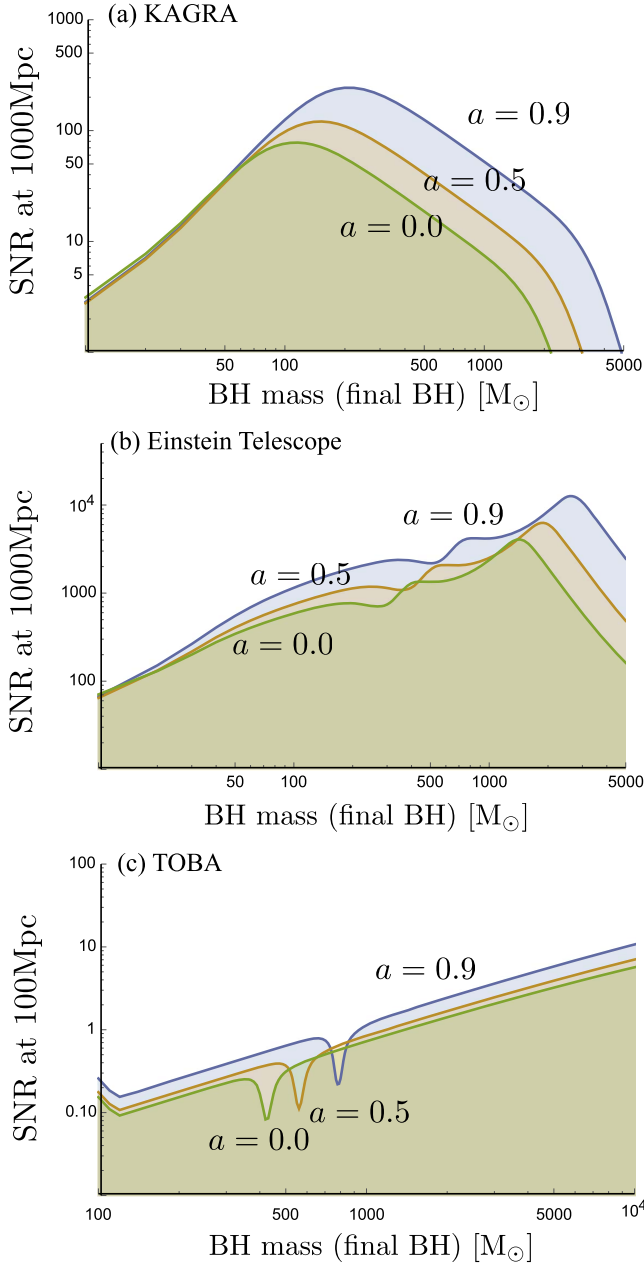


Figure 7. S/N for ring-down waves from a BH with spin parameter a , which appears at a distance of 1 Gpc. Panels (a) and (b) are for KAGRA and the Einstein Telescope, respectively. We see that ring-down frequencies of IMBHs (especially for 100–400 M_\odot) are the best target for both KAGRA and the Einstein Telescope. Panel (c) is for TOBA, and the distance is estimated at 100 Mpc.

Up to here, we see that the S/N is larger when the BH spin a is large, and it reaches a maximum when $m_1 = m_2$.

In Figure 7, we plot the S/N of ring-down waves from a BH at a distance of 1 Gpc at KAGRA for $A = 0.4$. The results depend on the BH spin parameter a , but we see that ring-down frequencies of IMBHs (especially for 100–400 M_\odot) are the best target for both KAGRA and the Einstein Telescope.

3.3. Detectable Distance

By specifying the BH mass and spin, together with ρ , we can then find the distance d_L that satisfies Equation (25). We call this distance the detectable distance, $D(M, a, \rho)$.

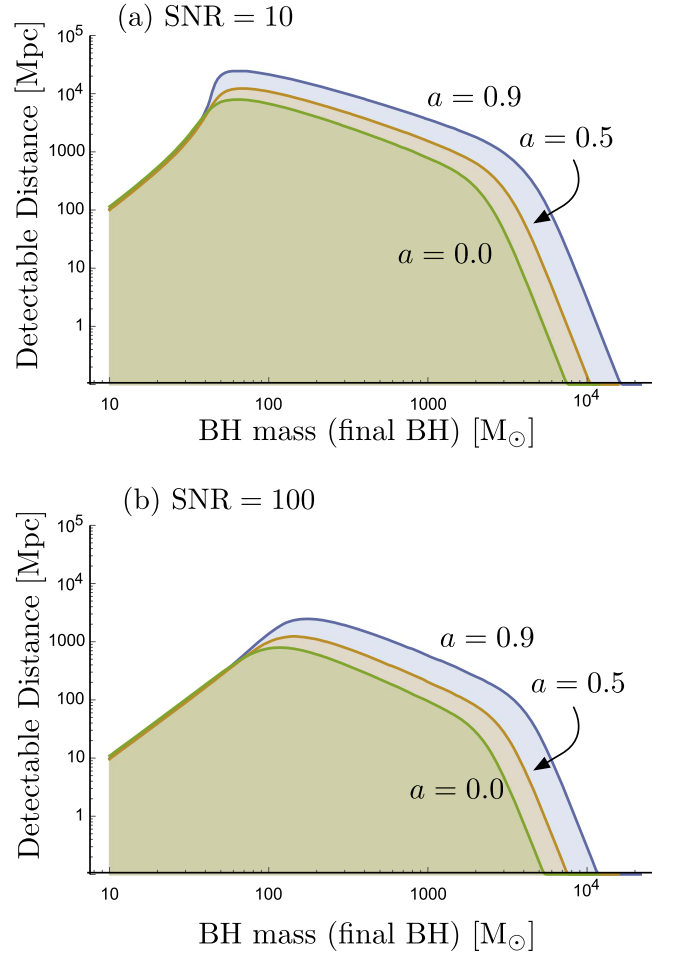


Figure 8. Detectable distance D of the ring-down signal at KAGRA. S/N is set to (a) 10 and (b) 100.

We converted Figure 7 into the plots of detectable distance D with a function of BH mass M for S/N = 10 and 100. We show them in Figure 8 for KAGRA. We see that the designed KAGRA covers at least 100 (10) Mpc at S/N = 10 (100) for $10 M_\odot < M$, and KAGRA covers 1 Gpc at S/N = 10 for $40 M_\odot < M < 1000 M_\odot$.

4. Event Rate

Using the detectable distance $D(M, a, \rho)$ obtained in the previous section, we set the upper limit of z for integrating Equation (10) to obtain the number of galaxies, N_{galaxy} , and then obtain the number of BH mergers, N_{merger} , according to the procedure shown in Section 2. We show N_{merger} in Figures 9(a1) and (b1) for S/N = 10 and 30, respectively.

The event rate R , then, is estimated by Equation (16). We show them in Figures 9(a2) and (b2). Previous works (e.g., Miller 2002; Will 2004) assume that the number of events to the merger sources is $\sim 10^{-10}$, which can be seen in our Figures 9(a1) and (a2) for higher-spinning BH cases.

Figure 9 is for specifying the BH spin parameter a , but if we assume that a is homogeneously distributed, then the averaged R is estimated as in Figure 10.

The event rate versus mass distribution of Figure 10 has its peak $R \sim 7.13$ [yr] at $M \sim 59.1 M_\odot$ (200–375 [Hz]) for $a = 0-0.9$. It is interesting to find out that this peak mass matches the final BH mass of GW150914. The mergers of the

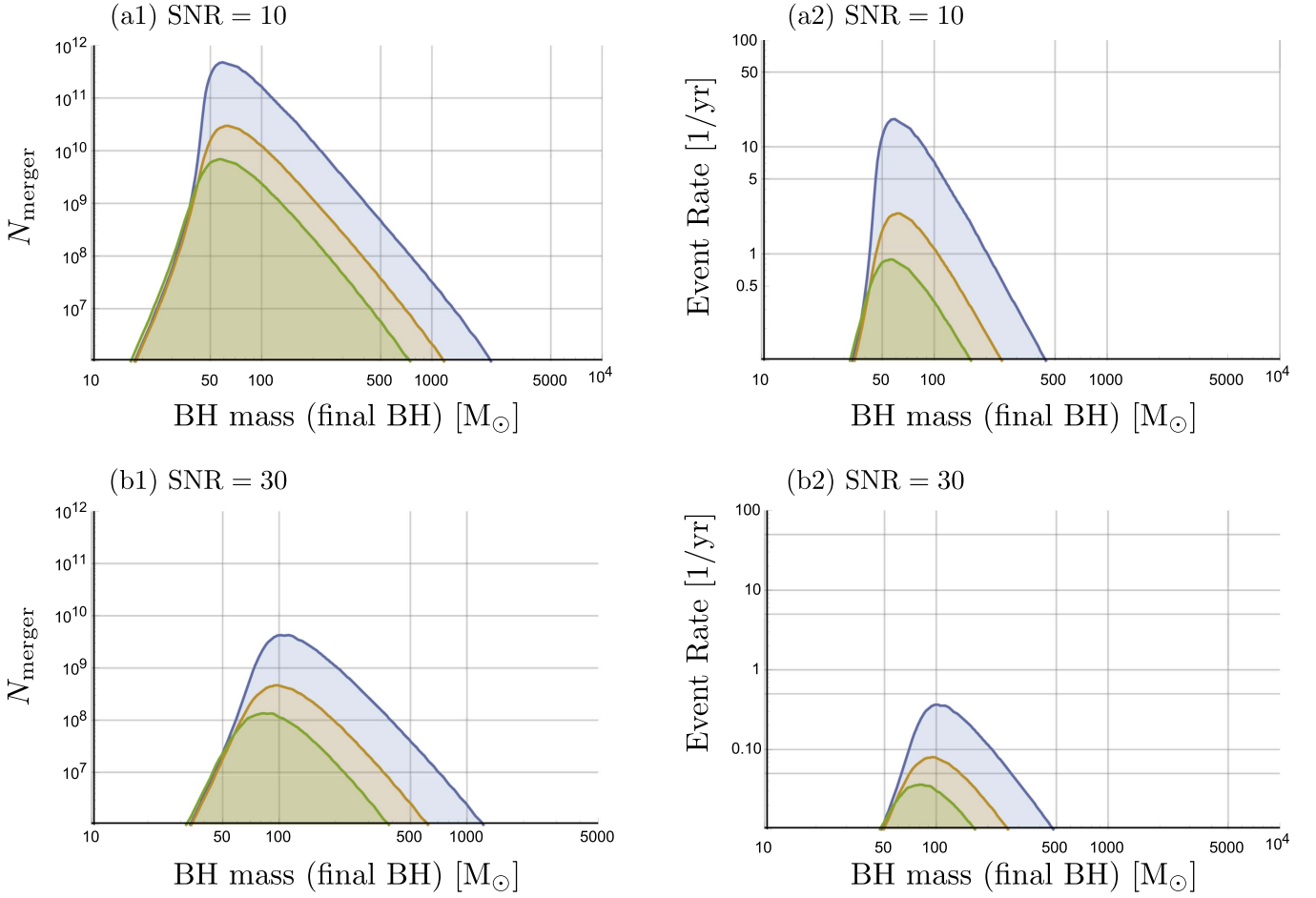


Figure 9. Number of BH mergers within the detectable distances (a1, b1) and event rate R (a2, b2) as a function of BH mass M with $S/N \rho = 10$ and 30 for KAGRA. Three distributions for each figure are of $a = 0.9, 0.5,$ and 0.0 (from largest to lowest), respectively.

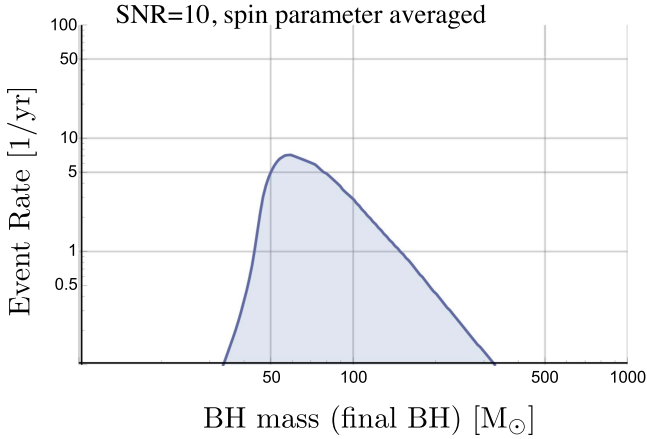


Figure 10. Event rate R as a function of BH mass M with $S/N \rho = 10$ for KAGRA. Spin parameter dependences are averaged.

range above $R > 1$ [1/yr] have mass $40M_{\odot} < M < 150M_{\odot}$. The total number of events above $R > 1$ [1/yr] is ~ 211 .

Our event rate sounds similar to that of other groups. For example, the LIGO-Virgo group updated their estimated event rates after the detection of GW150914 as $2\text{--}600 \text{ Gpc}^3 \text{ yr}^{-1}$ assuming BH mass distribution models as flat or power law ($\sim M^{-2.35}$; Abbott et al. 2016d). Kinugawa et al. (2014) estimate $70\text{--}140 \text{ yr}^{-1}$ from their Population III model. Inoue et al. (2016) estimate $< 60 \text{ yr}^{-1}$ from their BH merger model

inferred from the luminosity function of ultraluminous X-ray sources. However, our model predicts BH mergers with $M > 100 M_{\odot}$, which will be a key to test our model in the future.

5. Summary

Based on a bottom-up formation model of an SMBH via IMBHs, we estimate the expected observational profile of gravitational waves at ground-based detectors. We simply modeled that cores of molecular clouds become BHs if they are more than $10 M_{\odot}$, which become building blocks for forming larger BHs. We also modeled that BH mergers are accumulations of equal-mass ones and suppose that these occur hierarchically. We did not include gas accretion after a BH is formed.

At the designed KAGRA (or equivalent advanced LIGO/VIRGO), with the most standard criterion of the $S/N \rho = 10$, we find that the mass distribution of BH mergers has its peak at $M \sim 60 M_{\odot}$, and we can detect also BHs in the range $40 M_{\odot} < M < 150 M_{\odot}$ in certain event rates.

Detailed numbers depend, of course, on model settings and model parameters. We assume that all the galaxies in the universe evolve in the single scenario, which will overestimate the event rate if some SMBHs are formed from the direct collapse of gas clouds. We also ignore galaxy mergers, which are another route of forming SMBHs. These issues will lower the merger event rates, so that our event rates can be

understood at the maximum number. However, the profiles of event rates in terms of BH mass (Figure 10) will remain the same; therefore, our model's feature, the existence of gravitational-wave events with BHs larger than $100 M_{\odot}$, will be tested by accumulating actual events.

We conclude that the statistics of the signals will give us both a galaxy distribution and a formation model of SMBHs, as well as in the future cosmological models/gravitational theories.

We thank the anonymous referee for constructive suggestions. This work was supported in part by the Grant-in-Aid for Scientific Research Fund of the JSPS (C) No. 25400277 (H.S.), and also by MEXT Grant-in-Aid for Scientific Research on Innovative Areas "New Developments in Astrophysics Through Multi-Messenger Observations of Gravitational Wave Sources" (No. 24103005) (N.K.).

References

- Abbott, B., et al. (LIGO Scientific Collaboration and Virgo Collaboration) 2016a, *PhRvL*, **116**, 061102
- Abbott, B., et al. (LIGO Scientific Collaboration and Virgo Collaboration) 2016b, *PhRvL*, **116**, 241103
- Abbott, B., et al. (LIGO Scientific Collaboration and Virgo Collaboration) 2016c, *PhRvX*, **6**, 041015
- Abbott, B., et al. (LIGO Scientific Collaboration and Virgo Collaboration) 2016d, *ApJL*, **833**, 1
- Amaro-Seoane, P., & Santamaría, L. 2010, *ApJ*, **722**, 1197
- Ando, M., Ishidoshiro, K., Yamamoto, K., et al. 2010, *PhRvL*, **105**, 161101
- Baumgardt, H., & Makino, J. 2003, *MNRAS*, **340**, 227
- Begelman, M. C., Rossi, E. M., & Armitage, P. J. 2008, *MNRAS*, **387**, 1649
- Begelman, M. C., Volonteri, M., & Rees, M. J. 2006, *MNRAS*, **370**, 289
- Belczynski, K., Daniel, E. H., Tomasz, B., & O'Shaughnessy, R. 2016, *Natur*, **534**, 512
- Belczynski, K., Tomasz, B., & Bronislaw, R. 2004, *ApJL*, **608**, L45
- Berti, E., Cardoso, V., & Will, C. M. 2006, *PhRvD*, **73**, 064030
- Bond, J. R., & Carr, B. J. 1984, *MNRAS*, **207**, 585
- Bromm, V., & Loeb, A. 2004, *NewA*, **9**, 353
- Conselice, C. J., Wilkinson, A., Duncan, K., & Mortlock, A. 2016, *ApJ*, **830**, 83
- Ebisuzaki, T., Makino, J., Tsuru, T. G., et al. 2001, *ApJL*, **562**, L19
- Echeverria, F. 1980, *PhRvD*, **40**, 3194
- Finn, L. S., & Chernoff, D. F. 1993, *PhRvD*, **47**, 2198
- Flanagan, É. É., & Hughes, S. A. 1998, *PhRvD*, **57**, 4535
- Fregeau, J. M., Larson, S. L., Coleman Miller, M., O'Shaughnessy, R., & Rasio, F. A. 2006, *ApJL*, **646**, L135
- Fujii, M. S., Iwasawa, M., Funato, Y., & Makino, J. 2008, *ApJ*, **686**, 1082
- Fujii, M. S., & Portegies Zwart, S. 2015, *MNRAS*, **449**, 726
- Gair, J. R., Mandel, I., Coleman Miller, M., & Volonteri, M. 2011, *GRGr*, **43**, 485
- Greene, J. 2012, *NatCo*, **3**, 1304
- Haiman, Z. 2013, *The First Galaxies*, Vol. 396, ed. T. Wiklund, B. Mobasher, & V. Bromm, 293, arXiv:1203.6075
- Haiman, Z., & Loeb, A. 2001, *ApJ*, **552**, 459
- Inoue, Y., Tanaka, Y. T., & Isobe, N. 2016, *MNRAS*, **461**, 4329
- Inutsuka, S., Inoue, T., Iwasaki, K., & Hosokawa, T. 2015, *A&A*, **580**, A49
- Ishidoshiro, K., Ando, M., Takamori, A., et al. 2011, *PhRvL*, **106**, 161101
- Iwasawa, M., An, S., Matsubayashi, T., Funato, Y., & Makino, J. 2010, arXiv:1011.4017
- Johnson, J. L., Whalen, D. J., Fryer, C. L., & Li, H. 2012, *ApJ*, **750**, 66
- Johnson, J. L., Whalen, D. J., Li, H., & Holz, D. E. 2013, *ApJ*, **771**, 116
- King, A. 2003, *ApJL*, **596**, L27
- Kinugawa, T., Miyamoto, A., Kanda, N., & Nakamura, T. 2016, *MNRAS*, **456**, 1093
- Kinugawa, T., Inayoshi, K., Hotokezaka, K., Nakauchi, D., & Nakamura, T. 2014, *MNRAS*, **442**, 2963
- Leaver, E. W. 1985, *RSPSA*, **A402**, 285
- Loeb, A., & Rasio, F. A. 1994, *ApJ*, **432**, 52
- Marchant, A. B., & Shapiro, S. L. 1980, *ApJ*, **239**, 685
- Matsubayashi, T., Makino, J., & Ebisuzaki, T. 2007, *ApJ*, **656**, 879
- Matsubayashi, T., Shinkai, H., & Ebisuzaki, T. 2004, *ApJ*, **614**, 864 (Paper I)
- Matsumoto, H., Tsuru, T. G., Koyama, K., et al. 2001, *ApJL*, **547**, L25
- Matsushita, S., Kawabe, R., Matsumoto, H., et al. 2000, *ApJL*, **545**, L107
- McConnell, N. J., & Ma, C. P. 2013, *ApJ*, **764**, 184
- Miller, M. C. 2002, *ApJ*, **581**, 438
- Nakano, H., Tanaka, T., & Nakamura, T. 2015, *PhRvD*, **92**, 064003
- Portegies Zwart, S. F., Holger, B., Piet, H., Makino, J., & McMillan, S. L. W. 2004, *Natur*, **428**, 724
- Portegies Zwart, S. F., Makino, J., McMillan, S. L. W., & Hut, P. 1999, *A&A*, **348**, 117
- Portegies Zwart, S. F., & McMillan, S. L. W. 2000, *ApJL*, **528**, L17
- Portegies Zwart, S. F., & McMillan, S. L. W. 2002, *ApJ*, **576**, 899
- Portegies Zwart, S. F., Baumgardt, H., McMillan, S. L. W., et al. 2006, *ApJ*, **641**, 319
- Rees, M. J. 1978, *Observatory*, **98**, 210
- Robertson, B. E., & Ellis, R. S. 2012, *ApJ*, **744**, 95
- Robertson, B. E., Ellis, R. S., Dunlop, J. S., McLure, R. J., & Stark, D. P. 2010, *Natur*, **468**, 55
- Sheth, R. K., & Tormen, G. 1999, *MNRAS*, **308**, 119
- Shibata, M., & Shapiro, S. L. 2002, *ApJL*, **572**, L39
- Sudou, H., Iguchi, S., Murata, Y., & Taniguchi, Y. 2003, *Sci*, **300**, 1263
- Tsuiji, M., Kitamura, Y., Miyoshi, M., et al. 2016, *PASJ*, **68**, L7
- Umehura, M., Loeb, A., & Turner, E. L. 1993, *ApJ*, **419**, 459
- Vale, A., & Ostriker, J. P. 2006, *MNRAS*, **371**, 1173
- Volonteri, M. 2012, *Sci*, **337**, 544
- Volonteri, M., & Begelman, M. C. 2010, *MNRAS*, **409**, 1022
- Will, C. M. 2004, *ApJ*, **611**, 1080
- Yagi, K. 2012, *CQGr*, **29**, 075005